

## Hot-pressing and mechanical properties of SiC ceramics with polytitanocarbosi- lane

Nobuhiro Hidaka<sup>a</sup>, Yoshihiro Hirata\*, Soichiro Sameshima and Hidekazu Sueyoshi

Department of Advanced Nanostructured Materials Science and Technology, Graduate School of Science and Engineering, Kagoshima University, 1-21-40 Korimoto, Kagoshima 890-0065, Japan

<sup>a</sup>Research Fellow of the Japan Society for the Promotion of Science

An SiC powder of median size 0.8  $\mu\text{m}$  was mixed with an  $\text{Al}_2\text{O}_3$  powder of median size 0.2  $\mu\text{m}$  in a 0.3 M- $\text{Y}(\text{NO}_3)_3$  solution at pH 5 to distribute homogeneously the sintering additives ( $\text{Al}_2\text{O}_3+\text{Y}^{3+}$  ions) around the SiC particles. In a 30 vol% SiC suspension, the network structure of SiC particles was formed by the heterocoagulation through the adsorbed  $\text{Al}_2\text{O}_3$  and  $\text{Y}^{3+}$  ions. The aqueous suspension of the SiC- $\text{Al}_2\text{O}_3$  (1.17 vol%)- $\text{Y}^{3+}$  ions (0.94 vol%  $\text{Y}_2\text{O}_3$ ) system was consolidated by filtration through a gypsum mold and formed green compacts of 52-55% of theoretical density. Polytitanocarbosi-lane (PTC) of 0.04-5.2 vol% was infiltrated into the calcined SiC compact. The SiC compacts with and without PTC were hot-pressed under a pressure of 39 MPa at 1950°C in an Ar atmosphere. Addition of PTC to the SiC compact increased the sinterability, flexural strength and fracture toughness of SiC and suppressed the grain growth during the hot-pressing. The measured mechanical values of SiC with 1.3 vol% PTC were as follows: average four-point flexural strength 711 MPa, fracture toughness 5.9  $\text{MPa}\cdot\text{m}^{1/2}$ , Vickers hardness 19-21 GPa, and Weibull modulus 12.5.

**Key words:** Silicon carbide, Polytitanocarbosi-lane, Hot-pressing, Mechanical properties.

### Introduction

Silicon carbide (SiC) is potentially useful as a high temperature structural material because of its high strength, high hardness, high creep resistance, and high oxidation resistance. Recently the chemical methods for the addition of sintering additives such as  $\text{Al}_2\text{O}_3$  plus  $\text{Y}_2\text{O}_3$  to SiC powder have been studied to control the liquid phase sintering and the resultant micro-structures of SiC ceramics [1-7]. Liden *et al.* [1] mixed 0.45  $\mu\text{m}$ -SiC powder with 2 mass%  $\text{Al}_2\text{O}_3$  (50 nm)-1 mass%  $\text{Y}_2\text{O}_3$  (10 nm) powders in aqueous solutions and sintered a dried green compact of 51% theoretical density to 99.7% relative density by sintering at 1880°C for 4 h in an Ar atmosphere. Mulla and Krstic [8] studied the densification of 0.5  $\mu\text{m}$ -SiC powder with 6-10 vol% of  $\text{Al}_2\text{O}_3$  plus  $\text{Y}_2\text{O}_3$  at 1800°-2000 °C for 5 minutes in an Ar atmosphere. The starting powders were mixed by attrition milling in ethyl alcohol using high-purity  $\text{Al}_2\text{O}_3$  balls. The dried and sieved powders were compacted by uniaxial pressing at a pressure of 200 MPa. These SiC compacts were sintered to a density higher than 97% theoretical density at 1850 °C. Sciti and Bellosi [9] studied the densification of SiC powder of 11.6  $\text{m}^2\text{g}^{-1}$  specific surface area by hot-

pressing under a pressure of 30 MPa at 1880 °C in vacuum. The SiC powder, 2.2-4.8 vol%  $\text{Al}_2\text{O}_3$  and 1.6-2.6 vol%  $\text{Y}_2\text{O}_3$  powders were mixed by a pulsed ultrasonic method in ethyl alcohol, and dried at 80 °C using a rotary evaporator. The dried and sieved powder started densification at 1470°-1520 °C and was sintered to a density higher than 98% at 1880 °C. The sinterability of the SiC- $\text{Al}_2\text{O}_3$ - $\text{Y}_2\text{O}_3$  system depends on the amount and ratio of  $\text{Al}_2\text{O}_3$ - $\text{Y}_2\text{O}_3$  additives [8-20]. The densification of SiC progresses through the dissolution-precipitation mechanism of SiC in the liquid phase of the  $\text{SiO}_2$ - $\text{Al}_2\text{O}_3$ - $\text{Y}_2\text{O}_3$  system. The  $\text{SiO}_2$  component is naturally formed on the surface of the as-received SiC powder. The chemical methods of dispersing SiC with the sintering additives are expected to provide the following advantages: (1) a homogeneous distribution of the additives around SiC particles, (2) an increased densification rate by the well-distributed liquid and (3) a decrease of the amount of additives needed [21].

In our previous papers [6, 7], the interaction of the silicon carbide-alumina- yttrium ion system in an aqueous suspension was investigated in order to disperse homogeneously the sintering additives around SiC particles. The addition of positively charged  $\text{Al}_2\text{O}_3$  (1.17 vol%) plus  $\text{Y}^{3+}$  ions (0.94 vol%  $\text{Y}_2\text{O}_3$ ) to negatively charged SiC particles in an aqueous solution at pH 5 created a heterocoagulation and gave a homogeneous distribution of sintering additives around the SiC particles. The hot-pressing of consolidated SiC compacts under a pressure of 39 MPa at 1850°-1950 °C gave dense SiC ceramics

\*Corresponding author:  
Tel : +81-99-285-8325  
Fax: +81-99-257-4742  
E-mail: hirata@apc.kagoshima-u.ac.jp

(95-99% of theoretical density) with excellent mechanical properties: average four-point flexural strengths of 565-666 MPa, fracture toughness of 5.0-6.5 MPa·m<sup>1/2</sup> and Vickers hardness of 19-21 GPa. On the other hand, we reported the formation of nanometer-sized SiC particles at 1500°-1750 °C in an Si-Ti-C-O fiber prepared from polytitanocarbosilane (PTC). This type of fine particle has a higher solubility in a given liquid than submicrometer-sized particles [22]. The use of nanometer-sized SiC particles is expected to reduce the sintering temperature and achieve a dense fine microstructure because of their high solubility in the liquid made from the oxide additives. From the above viewpoint, the influence of PTC addition on the densification, microstructures and mechanical properties of the SiC with Al<sub>2</sub>O<sub>3</sub> and Y<sub>2</sub>O<sub>3</sub> was studied at 1950 °C in an Ar atmosphere.

### Experimental Procedure

An  $\alpha$ -SiC powder with the following characteristics (supplied by Yakushima Electric Industry Co., Ltd., Kagoshima, Japan) was used in this experiment: chemical composition, SiC 98.90 mass%, SiO<sub>2</sub> 0.66 mass%, C 0.37 mass%, Al 0.004 mass%, Fe 0.013 mass%, median size 0.8  $\mu$ m, specific surface area 13.4 m<sup>2</sup>/g (diameter of equivalent spherical particle 0.14  $\mu$ m). As a sintering additive, a submicrometer-sized  $\alpha$ -Al<sub>2</sub>O<sub>3</sub> powder with the following properties was mixed with the as-received SiC powder: chemical composition >99.99% Al<sub>2</sub>O<sub>3</sub>, median size 0.2  $\mu$ m, specific surface area 10.5 m<sup>2</sup>/g (Sumitomo Chemical Industry Co., Ltd., Tokyo, Japan). The zeta potentials of  $\alpha$ -SiC and  $\alpha$ -Al<sub>2</sub>O<sub>3</sub> powders were measured as a function of pH at a constant ionic strength of 0.01 M-NH<sub>4</sub>NO<sub>3</sub> and are shown in Fig. 1 (Rank Mark II, Rank Brothers Ltd., Cambridge, UK). The electrophoretic mobility of the particles was measured twenty times at each pH and converted to the zeta potential. In this experiment, the as-received  $\alpha$ -SiC powder was mixed with the  $\alpha$ -Al<sub>2</sub>O<sub>3</sub> powder at 30 vol% solids in a 0.3 M-Y(NO<sub>3</sub>)<sub>3</sub> aqueous solutions at pH 5.0. The volume ratio of the SiC/Al<sub>2</sub>O<sub>3</sub>/Y<sub>2</sub>O<sub>3</sub> components was adjusted to 1/0.0117/0.0094 (1/0.0145/0.0145 mass ratio). 0.01 M-HNO<sub>3</sub> and 0.01 M-NH<sub>4</sub>OH solutions were used for pH adjustment. The suspensions of the SiC-Al<sub>2</sub>O<sub>3</sub>-Y<sup>3+</sup> ion system were stirred by a magnetic stirrer for 12 h. The suspensions were consolidated by filtration through a gypsum mold and the consolidated powder compacts were calcined at 800 °C for 1 h in an Ar atmosphere. Polytitanocarbosilane (chemical composition (mass%), Si 44, Ti 2, C 42, H 9, O 3, molecular weight 15000 (Ube Industry, Ube)) was dissolved in a xylene solution at 0.01-50 mass% and infiltrated into the green compact under vacuum. The infiltrated sample then was heated to 170 °C in air to cure the polytitanocarbosilane. The cured samples were hot-pressed under a pressure of 39

MPa at 1950 °C for 2 h in an Ar flow. The heating and cooling rates were 10 K minute<sup>-1</sup>.

The densities of the green and sintered samples were measured by the Archimedes method using kerosene. The surface of sintered SiC ceramics was polished with 1  $\mu$ m diamond paste and etched with a mixture of NaCl/NaOH=85/15 (molar ratio) at 800 °C for 20 minutes in air to observe the microstructures by a scanning electron microscope (SM300, Topcon Technologies, Inc., Tokyo, Japan). The hot-pressed samples were cut into specimens with sizes of 3 mm height, 4 mm width and 38 mm length. The specimens were polished with SiC papers of Nos. 600 and 2000 and 6 and 1  $\mu$ m diamond paste. The Vickers hardness of the hot-pressed SiC was measured at a load of 9.8 N. The flexural strength of SiC was measured at room temperature by a four-point flexural method over spans of 30 mm (lower span) and 10 mm (upper span) at a crosshead speed of 0.5 mm/minute. The strain gauge was attached on the tensile plane of the specimen to measure the Young's modulus. The fracture toughness was evaluated by a single-edge V-notch beam (SEVNB) method. A thin diamond blade 1mm thick, where the tip of the V-notch had a curvature radius of 20  $\mu$ m, was used to introduce a V-notch of a/W=0.1-0.6 (a: notch length, W: width of the beam). The strength of the notched specimen was measured by three-point loading over a span of 30 mm at a crosshead speed of 0.5 mm/minute. Equation (1) provides the fracture toughness and equation (2) indicates the shape factor (Y) of the crack at S/W=7.5. S, P, and B in Eqs. (1) and (2) are the span width, applied load and thickness of the beam, respectively.

$$K_{IC} = \frac{3PS}{2BW^2} Y \sqrt{a} \quad (1)$$

$$Y = 1.964 - 2.837\lambda + 13.711\lambda^2 - 23.250\lambda^3 + 24.129\lambda^4 \quad (2)$$

$$\left( \lambda = \frac{a}{W} \right)$$

### Results and Discussion

#### Sintering of SiC

The zeta potentials in Fig. 1 support the electrostatic adsorption of Y<sup>3+</sup> ions on the negatively charged SiC surfaces at pH 5.0. On the other hand, no adsorption of Y<sup>3+</sup> ions on the positively charged alumina surfaces was measured in our previous paper [6]. The aqueous suspension of 30 vol% SiC with 1.17 vol% Al<sub>2</sub>O<sub>3</sub> and 0.94 vol% Y<sub>2</sub>O<sub>3</sub> (as Y<sup>3+</sup> ions) at pH 5.0 showed a non-Newtonian flow. The apparent viscosity increased with the sintering additives in the following order: no additive < Al<sub>2</sub>O<sub>3</sub> < Y<sup>3+</sup> ions < Al<sub>2</sub>O<sub>3</sub>+Y<sup>3+</sup> ions [6]. The measured viscosity was closely correlated to the particle size in the suspension. This result indicates that the network of dispersed SiC particles was formed through the heterocoagulation with positively charged Al<sub>2</sub>O<sub>3</sub>

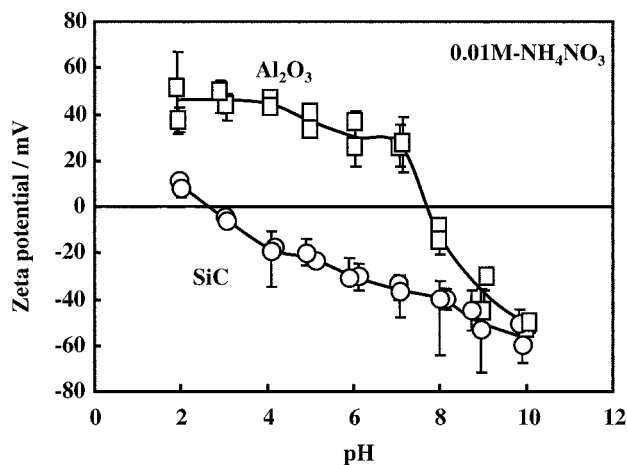


Fig. 1. Zeta potentials of SiC and  $\text{Al}_2\text{O}_3$  particles as a function of pH.

particles or  $\text{Y}^{3+}$  ions.

Figure 2 shows the relation between the density of SiC after the hot-pressing at  $1950^\circ\text{C}$  and the amount of PTC infiltrated. The amount of PTC was controlled by the concentration of the PTC-xylene solution. Compared with no infiltration of PTC, the addition of PTC enhanced the sinterability of SiC. The PTC infiltrated has excess carbon as compared with the chemical composition of SiC and TiC. Although some oxygen atoms are introduced in the PTC during the cure in air at  $170^\circ\text{C}$ , the oxygen atoms react with excess carbon to form CO gas at the hot-pressing temperature in an Ar atmosphere. The remaining carbon also reacts with the  $\text{Al}_2\text{O}_3$  or  $\text{Y}_2\text{O}_3$  additive to form volatile species ( $2\text{C} + \text{Al}_2\text{O}_3 \rightarrow \text{Al}_2\text{O} + 2\text{CO}$ ,  $2\text{C} + \text{Y}_2\text{O}_3 \rightarrow \text{Y}_2\text{O} + 2\text{CO}$ ) during the hot-pressing. These reactions reduce the

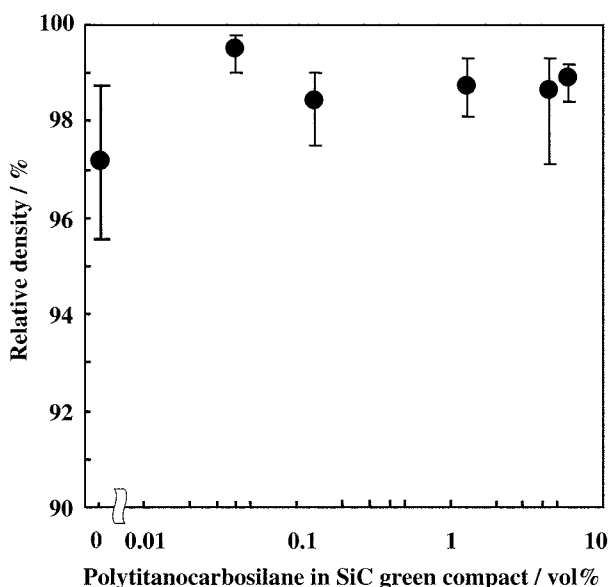


Fig. 2. Relationship between the density of SiC after the hot-pressing at  $1950^\circ\text{C}$  and the amount of PTC infiltrated into green SiC compacts.

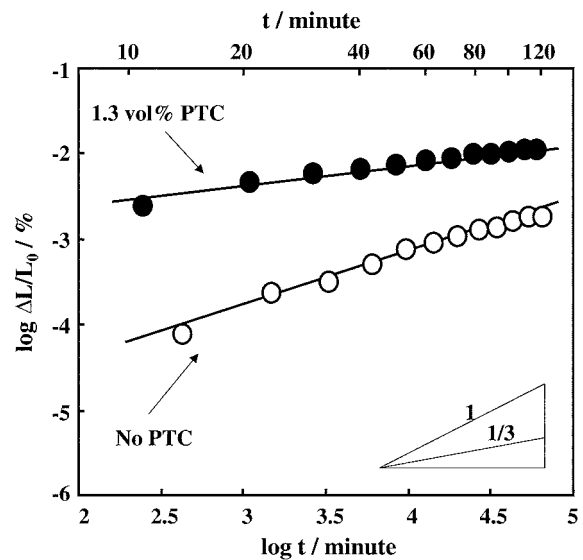


Fig. 3. Typical shrinkage of SiC with and without PTC during the hot-pressing at  $1950^\circ\text{C}$ .

mass of SiC with PTC, resulting in a decrease of the bulk density of hot-pressed SiC. However, the densification of SiC was accelerated by the infiltration of PTC, as seen in Fig. 2.

To analyze the sintering mechanism of SiC with PTC, the relationship between the shrinkage ( $\Delta L/L_0$ ) of a SiC compact based on the sample height ( $L_0$ ) for 0 h at  $1950^\circ\text{C}$  and hot-pressing time ( $t$ ) was plotted on log-log axes. The thermal expansion of the graphite die during the hot-pressing was calibrated in the analysis. Figure 3 shows the typical shrinkage of SiC with and without PTC during the hot-pressing at  $1950^\circ\text{C}$ . A good linear relation was observed in each SiC compact. The slope of the straight line in Fig. 3 is related to the mass transport mechanism of SiC. Figure 4 shows the slope ( $k$ ) for the  $\log(\Delta L/L_0)$ - $\log t$  plots as a function of the amount of PTC infiltrated. The following relationships between the mass transport mechanism and  $k$  value are proposed in the early stages of sintering:  $k=0.33$  for grain boundary diffusion or liquid phase sintering dominated by diffusion in liquid [23],  $k=0.40$  for bulk diffusion,  $k=0.50$  for liquid phase sintering dominated by dissolution-precipitation mechanism [23], and  $k=1.0$  for a viscous deformation mechanism [24]. As seen in Fig. 4, a high  $k$  value ( $0.69 \pm 0.01$ ) for the SiC without PTC decreased to  $0.36 \pm 0.10$  for the SiC with PTC. The measured results suggest that (1) the SiC compact without PTC was densified by mixed mass transport mechanisms of dissolution-precipitation and viscous deformation by the liquid phase of the  $\text{SiO}_2$ - $\text{Al}_2\text{O}_3$ - $\text{Y}_2\text{O}_3$  system formed at  $1950^\circ\text{C}$  and (2) densification of the SiC with PTC proceeded mainly by solid state sintering (grain boundary diffusion and bulk diffusion) or liquid phase sintering dominated by diffusion of SiC in the liquid of the  $\text{SiO}_2$ - $\text{Al}_2\text{O}_3$ - $\text{Y}_2\text{O}_3$  system. That is, the addition of PTC to SiC decreases

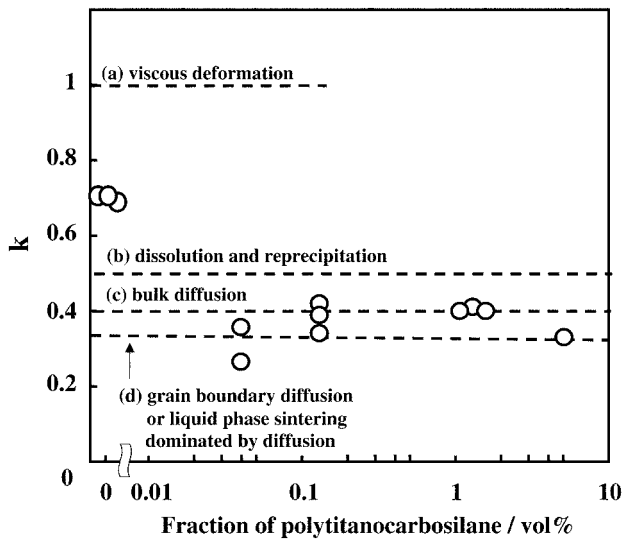


Fig. 4. Slope ( $k$ ) for the straight lines in Fig. 3 and the amount of PTC infiltrated.

the interfacial energy between SiC grains and also increases the bulk diffusion of Si or C atoms. The change of densification mechanisms with PTC, observed in Fig. 4, was effective in achieving a the high bulk density (Fig. 2).

#### Microstructures of hot-pressed SiC

Figure 5 shows the microstructures of SiC hot-pressed at 1950°C. The SiC with Al<sub>2</sub>O<sub>3</sub> (1.17 vol%) plus Y<sup>3+</sup> ions (0.94 vol% Y<sub>2</sub>O<sub>3</sub>) consisted of 0.8–10.8 μm grains (Fig. 5(a)). The median size of starting SiC particles was 0.8 μm. The densification of SiC was accompanied by grain growth (average 3.5 μm) through the oxide liquid. That is, the densification of SiC with Al<sub>2</sub>O<sub>3</sub> plus Y<sup>3+</sup> ions is explained by the enhanced mass transport in the liquid formed at the grain boundaries or related to the increased driving force for sintering due to the decreased interfacial energy at the grain boundaries. Figure 5(b)–(f) show the microstructures of the SiC with PTC. The average grain size, measured on 200 grains, was 3.3, 2.4, 2.3, 2.2 and 2.0 μm for the addition of PTC of 0.04, 0.13, 1.3, 5.1 and 5.2 vol%, respectively. The PTC addition has an effect on the formation of a fine microstructure in addition to the enhancement of the sinterability of SiC (Fig. 2).

#### Mechanical properties of hot-pressed SiC

The hot-pressed SiC showed a brittle fracture behavior with Young's moduli of 364–550 GPa. Figure 6 shows the mechanical strength (a) and fracture toughness (b) of SiC as a function of the amount of PTC infiltrated. The addition of PTC was effective in increasing the strength of SiC. The maximum strength reached 840 MPa in the case of SiC with 0.04 vol% PTC. On the other hand, no significant improvement of the strength was measured in the SiC with for 0.13 vol% PTC (total 7 specimens). The addition of PTC was also effective

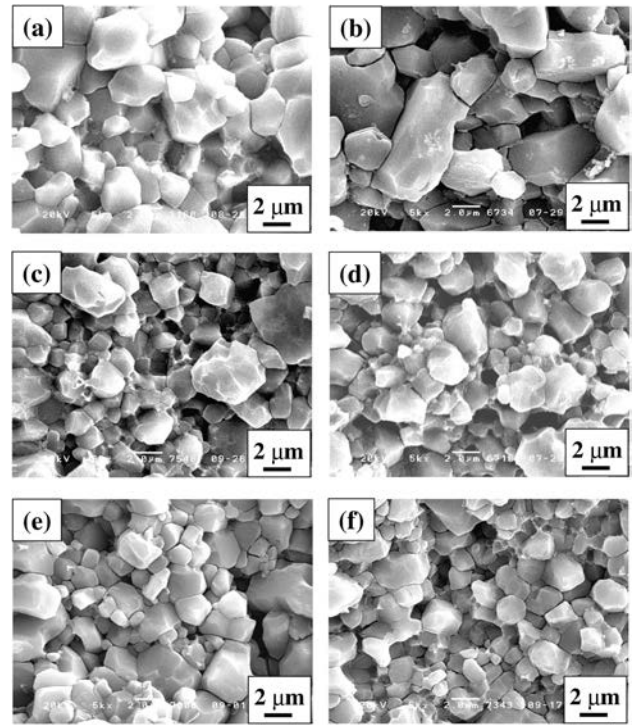


Fig. 5. Microstructures of the SiC hot-pressed with PTC of (a) 0, (b) 0.04, (c) 0.13, (d) 1.3, (e) 5.1 and (f) 5.2 vol%.

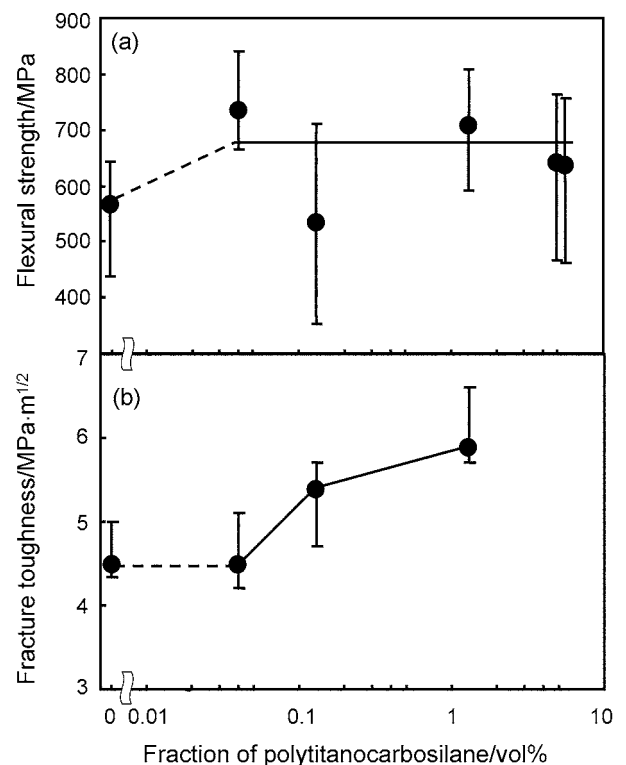


Fig. 6. Fracture strength (a) and fracture toughness (b) of hot-pressed SiC as a function of amount of PTC infiltrated.

in increasing the fracture toughness. The fracture toughness increased gradually with increasing PTC fraction and reached 5.9 MPa·m<sup>1/2</sup> in the SiC with 1.3 vol%

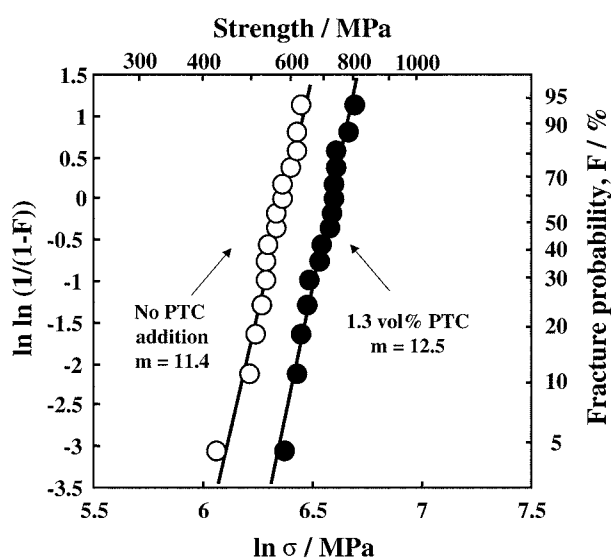


Fig. 7. Weibull plots of the strengths for SiC hot-pressed with and without PTC at 1950 °C.

PTC. The cracks formed by the Vickers indenter in the SiC hot-pressed with and without PTC propagated along the grain boundaries, causing crack deflection and bridging by grains. The increased fracture toughness with the addition of PTC may be explained by an increased interfacial strength at grain boundaries. As discussed in the previous Sections, the infiltrated PTC reacts with  $\text{Al}_2\text{O}_3$  and  $\text{Y}_2\text{O}_3$  additives and changes the properties of grain boundaries. The result in Fig. 6(b) suggests that PTC infiltration enhances the fracture resistance at grain boundaries.

The strength of brittle ceramic materials depends on the fracture toughness and size of flaw included. As mentioned above, excess carbon from PTC reacts with oxide additives ( $\text{Al}_2\text{O}_3$  and  $\text{Y}_2\text{O}_3$ ) to form volatile species. As a result, the direct bonding between SiC grains may increase the grain boundary strength, leading to the increased fracture toughness. This result in Fig. 6(b) can explain the increased strength in Fig. 6(a). Another factor is the decrease of flaw size. The flaw size is generally dominated by the grain size. As seen in Fig. 5, the grain size decreased with PTC addition. This result is favorable to increase the strength of SiC. Figure 7 shows the Weibull plots of flexural strength for the SiC with and without PTC. The strength at a failure probability of 50% and the Weibull modulus were 565 MPa and 11.4 for the SiC without PTC, and 711 MPa and 12.5 for the SiC with 1.3 vol% PTC, respectively. A PTC addition improved the reliability of the mechanical strength of SiC. The Vickers hardness of SiC at a load of 9.8 N was  $19 \pm 1$ ,  $18 \pm 3$ ,  $19 \pm 2$ ,  $21 \pm 5$ ,  $18 \pm 3$  and  $21 \pm 2$  GPa for the addition of PTC of 0, 0.04, 0.13, 1.3, 5.1 and 5.2 vol%, respectively. The addition of PTC showed no influence on the hardness of SiC.

## Conclusions

(1) The green SiC compact (53-55% of theoretical density) with oxide additives (1.17 vol%  $\text{Al}_2\text{O}_3$  plus 0.94 vol%  $\text{Y}_2\text{O}_3$ ) was hot-pressed at 1950 °C to 95-98% relative density by the mixed mass transport mechanisms of dissolution-precipitation and viscous deformation.

(2) Infiltration of PTC of 0.04-5.3 vol% into green SiC compacts with the oxide additives increased the sinterability of SiC during the hot-pressing by an enhanced mass transport mechanism associated with solid state sintering (grain boundary diffusion and bulk diffusion) or liquid phase sintering dominated by diffusion of SiC in the liquid of the  $\text{SiO}_2$ - $\text{Al}_2\text{O}_3$ - $\text{Y}_2\text{O}_3$  system.

(3) A PTC addition suppressed the grain growth of SiC during the hot-pressing.

(4) A PTC addition to a green SiC compact increased the mechanical strength, fracture toughness and Weibull modulus after the hot-pressing.

## References

1. E. Liden, E. Carlstrom, L. Eklund, B. Nyberg, and R. Calsson, *J. Am. Ceram. Soc.* 78 (1995) 1761-1768.
2. Y. Hirata, K. Miyano, S. Sameshima, and Y. Kamino, *Colloid and Surfaces, A: Physicochem. & Eng. Aspects* 133 (1998) 183-189.
3. Y. Hirata, S. Tabata, and J. Ideue, *J. Am. Ceram. Soc.* 86 (2003) 5-11.
4. Y. Hirata, K. Hidaka, H. Matsumura, Y. Fukushige, and S. Sameshima, *J. Mater. Res.* 12 (1997) 3146-3157.
5. S. Sameshima, K. Miyano, and Y. Hirata, *J. Mater. Res.* 13 (1998) 816-820.
6. N. Hidaka, Y. Hirata, and S. Sameshima, *J. Ceram. Proc. Res.* 3 (2002) 271-277.
7. N. Hidaka and Y. Hirata, *Ceram. Forum Inter.* submitted, 2003.
8. M.A. Mulla and V.D. Krstic, *Am. Ceram. Soc. Bull.* 70 (1991) 439-443.
9. D. Sciti and A. Bellosi, *J. Mater. Sci.* 35 (2000) 3849-3855.
10. L.M. Wang and W.C. Wei, *J. Ceram. Soc. Jpn.* 103[5] (1995) 434-443.
11. J.H. She and K. Ueno, *Mater. Chem. Phys.* 59 (1999) 139-142.
12. G. Magnani, G.L. Minocari, and L. Pilotti, *Ceram. Inter.* 26 (2000) 495-500.
13. V.D. Krstic, *Mater. Res. Soc. Bull.* XX[2] (1995) 46-49.
14. J.H. She and K. Ueno, *Mater. Res. Bull.* 34 (1999) 1629-1636.
15. S.K. Lee and C.H. Kim, *J. Am. Ceram. Soc.* 77 (1994) 1655-1658.
16. Y.W. Kim, J.Y. Kim, S.H. Rhee, and D.Y. Kim, *J. Eur. Ceram. Soc.* 20 (2000) 945-949.
17. V.V. Pujar, R.P. Jensen, and N.P. Padture, *J. Mater. Sci. Lett.* 19 (2000) 1011-1014.
18. S.-G. Lee, W.-H. Shim, J.-Y. Kim, Y.-W. Kim, and W.T. Kwon, *J. Mater. Sci. Lett.* 20 (2001) 143-146.
19. K.-S. Cho, H.-J. Choi, J.-G. Lee, and Y.-W. Kim, *J. Mater. Sci.* 36 (2001) 2189-2193.

20. J.-Y. Kim, H.-G. An, Y.-W. Kim, and M. Mitomo, *J. Mater. Sci.* 35 (2000) 3693-3697.
21. Y. Hirata and W.H. Shih, *Advances in Science and Technology* 14, Proceedings of 9th Cimtec-world Ceramics Congress, Ceramics: Getting into the 2000's-Part B Techna Srl., 1999, Edited by P. Vincenzini, p. 637-644.
22. Richard A. Swalin, *Thermodynamics of Solids* (John Wiley & Sons, Inc., New York, 1962) p. 148-152.
23. W.D. Kingery, *J. Appl. Phys.* 30[3] (1959) 301-306.
24. W.D. Kingery and M. Berg, *J. Appl. Phys.* 26[10] (1955) 1205-1212.